Investigating the morphological, mechanical and degradation properties of scaffolds comprising collagen, gelatin and elastin for use in soft tissue engineering

Chloe N. Grover[a*], Ruth E. Cameron[a], Serena M. Best[a]

[a] Department of Materials Science and Metallurgy, Cambridge Centre for Medical Materials, University of Cambridge, Pembroke Street, Cambridge CB2 3QZ, UK

Email: Chloe Grover (cng21@cam.ac.uk)

*Correspondence: Chloe N. Grover, Department of Materials Science and Metallurgy, Cambridge Centre for Medical Materials, University of Cambridge, Pembroke Street, Cambridge CB2 3QZ, UK. Telephone: +44 1223 362966, Fax: +44 1223 334366.

Abstract

Collagen-based scaffolds can be used to mimic the extracellular matrix (ECM) of soft tissues and provide support during tissue regeneration. To better match the native ECM composition and mechanical properties as well as tailor the degradation resistance and available cell binding motifs, other proteins or different collagen types may be added. The present study has explored the use of components such as gelatin or elastin and investigated their effect on the bulk physical properties of the resulting scaffolds compared to those made from pure collagen type I. The effect of altering the composition and crosslinking was evaluated in terms of the scaffold structure, mechanical properties, swelling, degradation and cell attachment. Results demonstrate that scaffolds based on gelatin had reduced tensile stiffness and degradation time compared with collagen. The addition of elastin reduced the overall strength and stiffness of the scaffolds, with electron microscopy results suggesting that insoluble elastin interacts best with collagen and soluble elastin interacts best with gelatin. Carbodiimide crosslinking was essential for structural stability, strength and degradation resistance for scaffolds of all compositions. In addition, preliminary cell adhesion studies showed these highly porous structures (pore size 130–160 μm) to be able to support HT1080 cell infiltration and growth. Therefore, this study suggests that the use of gelatin in place of collagen, with additions of elastin, can tailor the physical properties of scaffolds and could be a design strategy for reducing the overall material costs.

Keywords

Collagen; gelatin; elastin; mechanical properties; degradation

1. Introduction

Due to the limited availability of donor organs and tissues, intensive research has been conducted into the use of tailor-made biomaterials in tissue regeneration. Engineered tissue should have the capacity to become structurally integrated with the native tissue, providing support during the regeneration process but being able to biodegrade after it has served its function (Liu et al. 2007). 'Smart' biomaterials must provide an environment similar to the native extracellular matrix so as to encourage cells to generate new tissue and enhance repair. The requirements of such a scaffold are: 1) highly porous structures to allow cell and nutrient infiltration, 2) similar mechanical properties to the native tissue, 3) the ability to degrade to non-toxic products and 4) biocompatibility, allowing cells to attach and proliferate.

Scaffolds frequently used in tissue engineering have compositions based on the native extracellular matrix of soft tissues i.e. containing both collagen and elastin (Lee, Singla et al. 2001; van Luyn et al. 2002; Buttafoco et al. 2005; Xiang et al. 2006; Daamen et al. 2007; Daamen et al. 2008). Collagen typically gives the tissue its mechanical strength and stiffness, while elastin can provide elasticity and the ability to store elastic-strain energy. Collagen's relatively high tensile strength and stiffness (120 MPa and 1.2 GPa respectively when hydrated (Gosline et al. 2002)) means that even small changes in its concentration, type, crosslinking and spatial alignment in the ECM can lead to large effects on the mechanical properties of the tissue. Our research is concerned with myocardial engineering. Heart muscle has been shown to contain approximately 75–90% collagen and up to 25% elastin (dry weight), where the collagen is 60–85% type I and 15–40% type III (Lowry et al. 1941; Weber 1989; Bishop et al. 1990; Mukherjee and Sen 1991, 1993; Marijianowski et al. 1995; de Souza 2002). It should be noted, however, that each tissue has its own set and content of proteins and biomolecules, and thus attention should be paid to combining the appropriate proteins to provide the optimal physical properties and microenvironment for cells. Various different materials have been used to produce scaffolds for cardiac tissue engineering; collagen type I (van Luyn et al. 2002; Zimmermann et al. 2002), collagen and glycosaminoglycans (Xiang et al. 2006), gelatin (Gelfoam) (Li et al. 1999) and polymers (Fujimoto et al. 2007; Hidalgo-Bastida et al. 2007; Engelmayr et al. 2008). However, little consideration has been

given to how the composition or crosslinking may affect the physical properties of the scaffold.

The impairment of cardiac function with disease is associated with a change in the ECM composition, specifically the collagen content, crosslinking and type (Bishop et al. 1990; Norton et al. 1997; Debessa et al. 2001; Yamamoto et al. 2002; Koshy et al. 2003). Therefore we have chosen to investigate scaffolds based on type I collagen with/without 10% elastin (a lower bound for elastin composition in the heart) such that the elastin content may provide our scaffolds with a resilience and distensibility usually provided by type III collagen (Weber 1989; Fung 1993; Pauschinger et al. 1999; de Souza 2002). Our choice of elastin rather than type III collagen was also one of economical significance: currently, type III collagen is nearly 5000 times the cost of type I collagen (website Sigma Aldrich). This also led to our investigation of gelatin as a potential scaffold base; a thermally denatured collagen, easier to extract and prepare and thus more practical to use (Rosellini et al. 2009). The thermal denaturation may alter the physical properties of the material as well as the available cell bindings sites (Kozlov and Burdygina 1983; Elliott et al. 2002). It has also been discussed that enhanced collagen crosslinking can lead to stiffening of soft tissues. Crosslinking using carbodiimides, such as 1-ethyl-3-(3-dimethylaminopropyl) carbodiimide hydrochloride (EDC), is via carboxylic acid and amine groups on the proteins (both collagen and elastin) and has been shown to increase their degradation stability and mechanical properties (Jorge-Herrero et al. 1999; Hafemann et al. 2001; Buttafoco et al. 2005; Chiu et al. 2010). In the production of crosslinked scaffolds, the degree of crosslinking should be sufficient to provide resistance to degradation but not to exceed the mechanical properties of the native myocardium.

In this paper we test the hypothesis that varying the protein composition of scaffolds can provide a means of tailoring their mechanical and degradation properties. The overall aim was to investigate the cost-effective production of a scaffold, composed of combinations of macromolecules found in the ECM, with suitable structural, mechanical and degradation properties for use in myocardial tissue engineering. The potential for the development of a scaffold with structural integrity, bulk composition and mechanical properties similar to heart tissue (Young's modulus of 10–150 kPa in the physiological regime (Nagueh et al. 2004; Alter et al. 2008; Engelmayr et al.

2008; Zhong et al. 2009; Wang et al. 2010)) was investigated. Cell adhesion was also studied as a preliminary test to provide initial insight into whether a scaffold optimised for its physical properties could be used as a vector to deliver cells. Further work into the cell reactivity of these biomaterials is being carried out in our lab. These scaffold compositions could easily be tailored to provide tissue-specific scaffolds suitable for use in a range of applications such as dermal replacement or cartilage repair.

2. Materials and Methods

2.1 Materials

Collagen (bovine dermal type I, Coll) was purchased from DevroMedical, UK. Insoluble (IE) and soluble (SE) elastin (both from bovine neck ligament), gelatin (type B from bovine skin, Gel), acetic acid (2 M), 1-ethyl-3-(3-dimethylaminopropyl) carbodiimide hydrochloride (EDC) and N-hydroxy-succinimide (NHS) were purchased from Sigma Aldrich (UK). Dulbecos Modified Eagles Medium (DMEM, Gibco), phosphate buffered saline (PBS, Gibco), Foetal Calf Serum (FCS), penicillin and streptomycin were purchased from Invitrogen Life Sciences (UK). HT1080 human fibrosarcoma cells were obtained from the European Collection of Animal Cell Cultures, Porton Down, UK. Other reagents were all analytical grade, commercially available and used as received.

2.2 Preparation of Mixed Composition Scaffolds

In total, seven different scaffolds were prepared and are detailed in Table 1. Briefly, collagen with or without (±) elastin were swollen in 0.05 M acetic acid at 4 ± 2°C overnight to produce a 1% (w/v) protein suspension. The resulting suspension was homogenised on ice for 10 min at 9,500 rpm using an Ultra-Turrax VD125 (VWR International Ltd, UK). Air bubbles were removed from the suspension by centrifuging at 2,500 rpm for 5 min (Hermle Z300, Labortechnik, Germany).

Gelatin-based slurries could not be prepared by homogenisation. Dissolution of the powder required heating and homogenisation at high temperatures resulted in the formation of a foam. However, the solution began to gel at temperatures below approximately 15°C, so homogenisation could not be carried out at low temperatures either. Gelatin-based solutions, 1% (w/v), were instead prepared by dissolving gelatin

± elastin in 0.05 M acetic acid at 37–45ºC with stirring for 1 hour (h). The solutions were then cooled to room temperature with stirring.

The mixed collagen-gelatin 1:1 suspension was prepared by mixing a gelatin solution with a collagen slurry (both 1% w/v), before centrifuging. All suspensions were then poured into silicone trays (Lakeland, UK), to ensure ease of removal, and freeze-dried in a VirTis adVantage benchtop freeze-drier (Biopharma Process Systems, UK) using a cycle adapted from work by O'Brien *et al.* and Yang *et al.* (O'Brien et al. 2005; Yang et al. 2005). A constant cooling rate of 0.9°C/min to a final freezing temperature of -26ºC was used. The temperature was then held constant at -26ºC for 4 h. The ice phase was sublimed under vacuum (80 mTorr) at 0ºC over 27 hours.

2.3 Chemical Crosslinking

Scaffolds were chemically crosslinked using a water-soluble carbodiimide to increase their strength and degradation resistance. The carboxylic acid groups on the collagen, gelatin and elastin were activated by 1-ethyl-3-(3-dimethylaminopropyl) carbodiimide hydrochloride (EDC) in the presence of N-hydroxy-succinimide (NHS), so as to reduce the number of side reactions and therefore induce crosslinking with free primary amine groups (Pieper et al. 1999). Crosslinking was carried out with 1.150 g EDC and 0.276 g NHS per gram of scaffold (molar ratio EDC:NHS 5:2, as described in (Olde Damink et al. 1996)), using ethanol/water (75% v/v) as a solvent (Buttafoco et al. 2005; Xiang et al. 2006). After reaction for 2 h at room temperature, the scaffolds were washed twice in ethanol/water (75% v/v) followed by three times in deionised water for 30 min each before subsequent freeze-drying (as previously described in 2.2).

The change in pore size, volume and mass, due to crosslinking, were evaluated after freeze-drying using the following equations:

$$\text{Volume Shrinkage (\%)} = 100 \times \{(V_0 - V)/V_0\}$$

where V_0 is the volume of the scaffold before and V is the volume after crosslinking;

$$\text{Mass Loss (\%)} = 100 \times \{(m_0 - m)/m_0\}$$

where m_0 is the mass before and m is the mass after crosslinking.

The degree of scaffold crosslinking was assessed by determination of the amine group content of the scaffolds spectrophotometrically after using 2,4,6-trinitrobenzene sulfonic acid (Olde Damink et al. 1996).

2.4 Characterisation of the Scaffolds

2.4.1 Scanning Electron Microscopy (SEM)

SEM was used to analyse the scaffold morphology (pore size and porosity, as well as the interaction between components). Each sample was cut through the thickness of the scaffold (approximately 4–8 mm), as well as sectioning them in half (parallel to the top surface). Scaffold samples (cross-section, top and bottom surfaces) were mounted on stubs and sputtered with an ultrathin layer of platinum for 2 min at 20 mA. The scaffolds were studied with a JEOL-820 scanning electron microscope operating at 10 kV.

Image data was imported into ImageJ software for analysis. The average pore size was obtained by measuring the maximum and minimum diameter of 10 pores chosen at random throughout the central section of the samples, whilst the porosity was determined by calculating the fraction of the total area occupied by pores per image.

2.4.2 Mechanical Properties

Stress-strain analysis of scaffolds in tension and compression were performed by uniaxial measurements using a Hounsfield tester, equipped with a 5 N load cell. Tests were repeated for 9–12 samples to obtain mean data.

2.4.2.1 Tensile Tests

Rectangular sections were cut with a cross-sectional area of approximately 7 x 4 mm and hydrated in deionised water at room temperature for 1 h prior to testing. They were then clamped vertically, with a gauge length of 10 mm and tested at a constant rate of 6 mm min^{-1}. The thickness and width of the samples were measured accurately at three different positions using electronic callipers. All samples were stretched until failure. Stress was calculated by dividing the force generated during extension by the initial cross-sectional area.

The resulting stress-strain curves were used to calculate the Young's modulus (E) and stress at 20% strain (σ), and the failure strain for each of the different scaffold compositions.

2.4.2.2 Compression Tests

All compression tests were performed perpendicular to the plane of the scaffold disc. Cylindrical punches, of 5 mm diameter and thickness of 4–8 mm, were taken of the scaffolds and hydrated in deionised water at room temperature for 1 h prior to testing. The impermeable, unlubricated compression platens were lowered so as to contact the sample and produce a small, but detectable load (0.002 N). Samples were then compressed at a rate of 6 mm min^{-1} until a sharp increase in stress was detected (densification of the sample) when the tests were stopped. Stress-strain curves were plotted and used to calculate the compressive modulus and stress at a strain of 20% (to enable comparison with tensile data).

2.4.3 Swelling and Degradation Study

Due to the formation of intermolecular bonds, the fluid-binding capacity and degradation kinetics of the scaffolds are affected by crosslinking. Phosphate buffered saline (PBS, pH 7.4), a relevant biological buffer, was used in both swelling and degradation experiments. Tests were repeated with four parallel samples each.

2.4.3.1 Swelling and Fluid Uptake

Cylindrical samples (diameter 5 mm) were submerged in 1–2 ml PBS and incubated at 37 ºC for up to 14 days (d). After different time intervals (1 h, 24 h, 3 d, 7 d, 10 d, 14 d) samples were removed and the wet weight (m_w) and swollen weight (after drying between filter paper, m_{sw}) were determined. Scaffolds were then dried in a vacuum oven at 37 ºC until constant mass was reached (m_d), and two different measurements of their capacity to retain water were made:

1. The ability of the scaffold structure to absorb fluid (the material and the pores)

Fluid uptake of scaffold (%) = 100 x $\{(m_w - m_d) / m_d\}$

2. The swelling ability of the scaffold material itself (PBS from pores is removed)

Fluid uptake of scaffold material (%) = 100 x $\{(m_{sw} - m_d) / m_d\}$

The pH value of the PBS was measured after each time point using a pH meter.

2.4.3.2 Degradation Study

Cylindrical samples were weighed (m_p) and submerged in PBS as above. After different time intervals (1 h, 7 d and 14 d) samples were washed in a large volume of deionised water to remove buffer salts and dried on filter paper to remove excess water before freeze-drying. The final mass was recorded (m_d) and used to calculate the percentage weight loss:

Weight loss (%) = 100 x $\{(m_p - m_d)/ m_p\}$

SEM images of scaffolds were used to analyse the change in pore size, and compression testing was performed at each time interval. These tests were repeated with four parallel samples each.

2.4.4 Cell Adhesion Study

HT1080 cells derived from a human fibrosarcoma were used in this study as they are an adherent cell line that express general collagen-binding integrins and therefore are expected to adhere to our scaffolds. Scaffolds were cut to approximate cuboids (7 x 7 x 5 mm) and sterilised by washing twice with 75% ethanol (10 min), rinsed three times with deionised water (10 min) and then washed with PBS before incubating with 0.5 ml supplemented-DMEM (10% FCS, 100 µg/ml penicillin and 100 µg/ml streptomycin) for 30 min at 37ºC. This medium was then removed and 10^5 HT1080 cells in 100 µl medium were seeded onto the scaffold cross-section and incubated for 20 min to allow them to attach. Scaffolds were then inverted and a further 10^5 cells in 100 µl medium were seeded onto the opposite surface. After a final 20 min incubation to allow cell attachment, 1 ml DMEM was added for culture for 3 d at 37 ºC under 5% CO_2.

After culture, scaffolds were rinsed with PBS (200 µl) and fixed with 4% paraformaldehyde in PBS (200 µl) for 30 min at room temperature, and finally washed three times with PBS. SEM images of the cell-seeded scaffolds were then taken.

2.4.5 Statistical Analysis

Results are expressed in the figures as mean ± standard error measurement. Student's t-test was used to compare differences among mean values of physical properties and post-hoc comparisons used Student Newman Keuls. Crosslinked samples were

compared with non-crosslinked samples of the same composition and a significant difference of $p \leq 0.05$ was denoted by *. Additionally, different composition were compared and a ■ indicates significant difference between compositions for statistical significance of $p \leq 0.05$.

3. Results

3.1 Scaffold Synthesis and Morphology

3.1.1 Synthesis

Samples produced were white in colour and had a porous structure that was encased in a film-like surface layer and base layer with a much smaller pore size. However, phase separation was noted in gelatin-insoluble elastin samples, where the dense, insoluble elastin fibres sank to the base of the scaffold and could be visually identified by their thick, fibre-like appearance and yellow colour. This was not observed in collagen-insoluble elastin samples, or samples containing soluble elastin. Although phase mixing to produce a homogeneous structure may have been expected for all samples, the effective mixing of components was only seen for collagen-insoluble elastin, gelatin-soluble elastin and collagen-gelatin scaffolds as depicted by the illustrations in Fig. 1.

3.1.2 Morphology and Effect of Crosslinking

The freeze-drying of slurries created matrices in which the pore size, shape and porosity varied throughout the cross-section in both crosslinked and non-crosslinked samples of all compositions. This change in pore shape and size is shown clearly in the SEM image of a crosslinked collagen scaffold (Fig. 2): larger pores in the central region (b), which decrease in diameter towards to bottom of the scaffold (c). The scaffold composition has little effect on the morphology of this central region, with a pore size of 130–160 μm and porosity of 65–75%. It should also be noted that the pore size and porosity also differ at the surfaces of the scaffolds (Fig. 2 d and e), with a film-like layer (porosity 15–30%) forming on the top surface and smaller pores on the bottom surface (60–110 μm, porosity 50–60%).

When scaffolds were crosslinked in ethanol/water (75% w/v) using EDC/NHS and subsequently freeze-dried, a porosity of approximately 70% was obtained,

significantly reduced compared with 90% before crosslinking and scaffolds shrank to up to 80% of their original volume (Table 2). These results are comparable to those for collagen scaffolds presented by other groups (Buttafoco et al. 2005 and Davidenko et al. 2010). The mass loss that occurred during the crosslinking process was only significant for collagen-soluble elastin scaffolds (11%, Table 2).

The physical mixing and interaction of elastin with collagen and gelatin can be seen in the SEM images and illustrations (Fig. 1, 3 and 4). At higher magnification, collagen fibre bundles of diameter 0.82 ± 0.16 μm can be seen within the sample cross-section (Fig. 3a, 4a). The gelatin samples were produced from a solution rather than fibrous suspension and thus the lack of fibres in the SEM images is to be expected (Fig. 3b, 4c). The insoluble elastin fibres (diameter 5.4 ± 0.84 μm) are homogeneously distributed throughout the collagen scaffold, although they tended to clump together in bundles containing up to ten elastin fibres (diameter 14.8 ± 1.59 μm). However, insoluble elastin sank to the bottom of gelatin scaffolds and was only visible in the SEM images of the bottom surface of the scaffold. There are no distinct phase-separated regions within the gelatin-soluble elastin scaffold (Fig. 4c), however globules of soluble elastin could be seen on the collagen fibres in both non-crosslinked and crosslinked samples (Fig. 4 a and b).

The value of free amine groups in all samples after crosslinking is lower than that prior to crosslinking, in the range of $4-9 \times 10^{-5}$ mol/g (Table 3). Collagen-based scaffolds showed a significantly lower degree of crosslinking (45−60%) compared with gelatin-based scaffolds (60−78%, $p \leq 0.05$). The non-crosslinked gelatin scaffolds had a higher number of free amine groups than the collagen samples.

3.2 Mechanical Testing

With regard to the physiological loading conditions of soft tissues, the mechanical properties of the scaffolds were examined in terms of their tensile modulus and strength at 20% strain (within the physiological regime of heart tissue (Nagueh et al. 2004; Alter et al. 2008; Wang et al. 2010)) and failure strain. Preliminary tests conducted on non-crosslinked scaffolds were unsuccessful due to low failure stresses and the difficulty of handling hydrated, non-crosslinked scaffolds. All subsequent

tests were conducted with fully hydrated, crosslinked scaffolds at room temperature and a rate of 6 mm min^{-1}.

3.2.1 Tensile Tests

The tensile stress-strain curves are typical of biological materials, in that they are all non-linear and J-shaped (Fig. 5), similar to those found for native extracellular matrix, in particular, myocardium (Nagueh et al. 2004; Wang et al. 2010). A comparison of the curves indicates that at low strains they follow that of native myocardium closely, but at strains greater than 10% the stiffness of the biomaterial scaffolds did not increase as rapidly. Since heart tissue operates in the physiological regime of up to 20% strain (Nagueh et al. 2004; Alter et al. 2008; Wang et al. 2010), and in order to easily compare results between different compositions, the stress and modulus were recorded at this point.

Scaffolds containing a higher percentage of collagen had a higher Young's modulus and strength at 20% strain (Table 4). The addition of less rigid elements, such as elastin or gelatin, reduces its stiffness to produce a curve that more closely matches that of the native myocardium in the low strain region. The use of gelatin alone produces a scaffold suitable at very low strains (less than 0.05%) but whose strength does not increase in line with that of the myocardium. The addition of elastin had a similar effect on both collagen and gelatin scaffolds in that there was a slight increase in strain at failure. These recorded strains at failure are underestimates due to the majority of scaffold failure occurring at the grips.

3.2.2 Compressive Tests

Distinct collapse plateau and densification regimes can be seen in the stress strain curves for scaffolds tested in compression (Fig. 6), regardless of the scaffold composition. These regions are characteristic of low density, open-cell foams (Harley et al. 2007). The initial linear elastic region is hard to identify, and it is likely that strut buckling and collapse occur at the same time.

In order to standardise the results, a comparison of the compressive modulus (E) and strength at a fixed strain (20%) was performed. The modulus and strength of the collagen-based scaffolds were reduced when tested in compression compared with in tension: for crosslinked collagen E_t=81 kPa whereas E_c=2.9 kPa and σ_t=7.8 kPa

whereas σ_c=0.4 kPa. In contrast, those properties of the gelatin-based scaffolds did not change significantly: for crosslinked gelatin E_t=4.6 kPa whereas E_c=4.25 kPa and σ_t=0.75 kPa whereas σ_c=1.0 kPa. The addition of elastin to either collagen or gelatin, resulted in a scaffold with reduced compressive strength and stiffness and a slight increase in strain at failure, as seen when testing in tension (Fig. 6).

3.3 Swelling and Degradation of Scaffolds

Effects of crosslinking and composition on the water binding capacity, swelling ability and degradation kinetics of the scaffolds were measured, as well as their mechanical properties in compression and pore structure.

3.3.1 Structure and Stability

The structural integrity of the scaffolds after water-uptake and degradation studies was confirmed by analysing the pore structure of samples, which were freeze-dried after incubation in PBS for 7 and 14 days. Initial observations of the scaffolds showed that non-crosslinked gelatin samples dissolved after less than an hours incubation in PBS. Whilst non-crosslinked collagen scaffolds survived incubation, after drying between filter paper to remove pore fluid the scaffolds collapsed; a stable structure could not be obtained even after rehydration. This meant that for non-crosslinked scaffolds, pore size analysis could not be conducted. Crosslinked scaffolds, however, showed no significant change in pore size after incubation in PBS for 14 days (results not shown).

3.3.2 Swelling and Fluid Uptake

The fluid binding capacity indicates the absorption of cell culture medium or physiologically relevant buffers during culture of cells. The PBS uptake of the scaffold structure and that of the material, give different measures of the ability of the scaffold to bind to fluids. The results are shown in Fig. 7, where the results for non-crosslinked gelatin-based samples are missing owing to the fact that these scaffolds dissolved after an incubation time of one hour.

Figure 7 shows that increased incubation time allows increased binding of the PBS to the scaffold material, demonstrating a time-dependent nature of swelling (Fig. 7 a and c). Although crosslinking results in a significant ($p \leq 0.05$) reduction of fluid uptake

by the scaffold material compared with non-crosslinked scaffolds, an increase in fluid uptake by the scaffold as a whole is seen (Fig. 7 b and d). The uptake of PBS into the bulk scaffold is found to be independent of time, with fluid uptake into the pores occurring almost instantaneously (represented by a single column on the graphs). For the scaffold itself, the hydrophilic nature of the material is likely to affect the quantity of PBS taken up by the scaffold material. Figure 8 shows that gelatin-containing scaffolds are able to take up more fluid into the material compared with the collagen scaffolds. A reduction in pH (from 7.4 to 6.5–6.8) was noted over the course of the study for all samples. After approximately three days this pH value reached a plateau and remained almost unchanged for the duration of the study.

3.3.3 Degradation Study

Degradation is likely to occur by dissolution of the scaffold struts exposed to PBS. The pore size of crosslinked scaffolds did not change, confirming that extensive degradation of the scaffold struts has not occurred. Mechanical properties of degrading samples were investigated in unconfined compression tests, using hydrated scaffolds. These tests could not be conducted on non-crosslinked samples due to the difficulty of handling the samples once hydrated (lack of structural stability).

It was found that: (1) The non-crosslinked gelatin-based scaffolds showed much faster degradation kinetics than all other scaffolds, with complete dissolution noted after incubation for 1 hour in PBS. (2) The greatest mass loss after 14 days was noted for the non-crosslinked samples (40% for collagen ± elastin scaffolds, up to 85% for collagen-gelatin samples and 100% for gelatin samples, data not shown). (3) Crosslinked scaffolds had a maximum mass loss of up to 15% for collagen-based and 25% for gelatin-based (Fig. 8). (4) The effect of adding elastin to collagen or gelatin on the scaffold mass loss was not significant within the overall error of the experiment (due to small changes in mass). (5) A statistically significant reduction in the compressive modulus at 20% strain was noted for all samples (except collagen-gelatin) over the 14 day incubation period.

The rate of mass loss slowed within the second week of testing (down to approximately 1% per day, except for gelatin-soluble elastin), with crosslinked samples retaining 75–95% of their original mass.

It should be noted that this swelling and degradation study was conducted in PBS (a biological buffer) in the absence of enzymes and with a different ionic composition to cell culture medium. It is known that collagen is degraded by collagenases and that the presence of cells (which secrete enzymes and other biomolecules) may alter the degradation kinetics of the scaffolds. As these scaffolds are intended for *in vivo* and *in vitro* use, it would be of interest to carry out degradation studies in the presence of enzymes or culture medium.

3.4 Cell Adhesion

Preliminary tests were conducted to establish whether crosslinked scaffolds could support cell adhesion and justify any further investigations into their potential use as cell delivery vehicles. These studies were conducted with adherent HT1080 cells, seeded onto the cross-section surface of crosslinked scaffold samples and cultured for 3 days. Seeding cells onto the cross-section reduced the effect of the surface film layer limiting the cell infiltration. SEM imaging of scaffolds showed that cells attached readily to both collagen- and gelatin-based scaffold surfaces, and in most cases showed clear spreading and attachment to the scaffold strut surface (Fig. 9). No significant differences in observed cell number were noted between scaffolds of different composition, but the 3-dimensional nature of the scaffolds made direct comparisons difficult. Longer-term culture was not investigated: after 3 days of culture cells started to form cell-cell contacts; these interactions may alter how the cells interact with the biomaterial. Our group is conducting further research into how the cells interact specifically with the biomaterial.

4. Discussion

The purpose of this study was to investigate the combination of alternative proteins, such as elastin (to replace type III collagen) and gelatin (as an alternative to type I collagen), for the production of a structurally stable scaffold with physical properties similar to that of native extracellular matrix, in particular the myocardium. Three main comparisons were made; crosslinked versus non-crosslinked, collagen versus gelatin and soluble versus insoluble elastin, and evaluated in terms of the structural, mechanical and degradation properties of the scaffolds.

4.1 Non-crosslinked versus crosslinked

Previous studies into the mechanical stiffness, strength and degradation stability of scaffolds have shown that these properties were increased after crosslinking (Jorge-Herrero et al. 1999; Hafemann et al. 2001; Buttafoco et al. 2005; Geutjes et al. 2007; Chiu and Radisic 2010; Chiu et al. 2010; Madhavan et al. 2010). Tests, conducted in this study, also confirmed these results: the mechanical testing of non-crosslinked scaffolds was difficult to conduct due to their low strength. The presence of cross-links (as confirmed by the TNBS assay) prevents chain sliding, providing mechanical strength and additional structural stability. Degradation studies in PBS demonstrated that non-crosslinked scaffolds had maximal mass loss, confirming that crosslinking is essential to prevent rapid dissolution/degradation of the scaffolds in aqueous environments and maintain their structural integrity. There is also the possibility of varying the degree of crosslinking so as to provide further control over the degradation kinetics.

Crosslinking of the scaffolds is required to obtain matrices that would resist degradation and mechanically support the heart during the pumping cycle (Jorge-Herrero et al. 1999; Hafemann et al. 2001; Buttafoco et al. 2005; Chiu et al. 2010; Davidenko et al. 2010). However, the crosslinking process should not alter the structure in such a way as to produce a detrimental effect on pore size, composition or biocompatibility. A small mass loss was noted during crosslinking for all scaffolds (except pure gelatin) and is likely to be as a result of dissolution of proteins from the scaffold struts by the crosslinking solution (Table 2). However, this mass loss was not considered significant, except in the case of collagen-soluble elastin (discussed later). A decrease in pore size of the central region e.g. from 190 to 160 μm for collagen and reduction in porosity (to ~ 70%) was also seen during crosslinking (Table 2). This may be as a result of the volume shrinkage and mass loss during crosslinking, as well as the formation of inter-fibre bonds. Some loss of pore structure is expected during the crosslinking process (hydration for 2 hours in ethanol/water) owing to mass loss and volume shrinkage. Additionally, the physical presence of the cross-links pulls fibres closer together and may cause a further reduction in the pore size, resulting in a more dense structure. The pore size is important in allowing cell infiltration, vascularisation and the diffusion of nutrients

and oxygen, and the scaffold porosity should be high to prevent obstruction of the material, which may lead to necrosis *in vivo* (Radisic and Vunjak-Novakovic 2005; Murphy et al. 2010). Although crosslinking reduces the pore size, these scaffolds were still able to support HT1080 cell infiltration and attachment (Fig. 9) and the pore size is within a range suitable for the growth of myocytes, endothelial cells and fibroblasts as reported in previous research (Gerdes et al. 1986; Radisic and Vunjak-Novakovic 2005; Wang et al. 2010).

During synthesis, a film-like layer forms over the top surface (Fig. 2 d) as a result of conduction in the freeze-drier (Harley et al. 2007) and a reduced pore size is visible on the bottom surface (Fig. 2 e) with occasional large voids (up to 180 μm), likely to be as a result of ice nucleation events on the silicone mould. If these materials were to be used for long-term cell culture experiments, the film-like top layer and small pore size on the base of the scaffold may act as barriers to nutrient and oxygen diffusion and may therefore need to be removed. Likewise, consideration should be given to the volume shrinkage of the scaffolds when crosslinking if these scaffolds are to be used for structurally sensitive devices. Further, it may be beneficial to investigate the production of scaffolds with aligned pores (rather than a random pore structure) where this specific feature may be favourable, such as in the myocardium.

The hydration of scaffolds is important in indicating how cell culture medium may be absorbed during culture and how the scaffold may behave *in vivo*. Crosslinking is known to reduce the hydrophilic nature of the material since groups involved in the binding of water are consumed during the crosslinking process (amino and carboxylic acid groups) (Charulatha and Rajaram 2003). Collagen-based scaffolds showed a reduced ability to uptake fluid after crosslinking (Fig. 7 a). However, due to the highly porous nature of the scaffold, the swelling ability of the material itself has little effect on the overall fluid retention (Fig. 7 b). Non-crosslinked scaffolds collapsed after incubation in PBS for just 1 hour (with gelatin scaffolds completely dissolving in this time period), whereas crosslinked scaffolds showed no significant change in pore size after 14 days. Even though there is a measured mass loss as a result of protein dissolution from the scaffold struts, the overall structure of crosslinked scaffolds remains stable and therefore they were able to hold more fluid compared with the mechanically weak non-crosslinked scaffolds. In spite of the fact that the pore size

and hydrophilic properties of the material may be reduced by the crosslinking process, crosslinking appears to be beneficial in achieving good absorption characteristics by providing structural stability to the bulk scaffold.

4.2 Collagen versus Gelatin

Collagen scaffolds showed a fibrous structure (Fig. 3 and 4) which resulted in J-shaped tensile stress-strain curves: initial large extensions for low applied load, then as the load is increased, the stiffness of the material increases due to a progressive alignment of the protein fibres (these are in agreement with previous research (Kim and Mooney 2000; Wang et al. 2010)). The gelatin used is produced by alkaline treatment of collagen that results in its denaturation and some loss of its triple helical, fibrous structure. It is this fibrous structure that gives collagen its strength and stiffness, enabling it to take up most of the load in native tissue (Fung 1993), and therefore we may expect that the gelatin samples have reduced tensile properties. It was indeed seen that gelatin samples have less of a J-shape and a lower strength and stiffness compared with collagen scaffolds. It should also be noted that the slight increase in the fluid uptake of gelatin scaffolds compared with collagen scaffolds (Fig. 10, indicating an increased hydrophilic nature) might have an effect on their mechanical properties.

The combination of collagen and gelatin resulted in a well-mixed scaffold (no signs of phase separation) whose tensile properties were most similar to that of the native myocardium at low strains (< 10%): stiffness at diastole (E=10–20 kPa) or systole (E=50–200 kPa (Nagueh et al. 2004; Alter et al. 2008; Engelmayr et al. 2008; Zhong et al. 2009; Wang et al. 2010)). It is the addition of the weaker gelatin that reduces the stiffness of the scaffold and brings its properties more in line with those of heart tissue. The 1:1 ratio of collagen to gelatin means that a more practical scaffold can be produced that has improved degradation resistance (compared to gelatin alone) and mechanical properties that are more suited to myocardial tissue engineering.

Since the scaffold may also be subjected to compressive loads during the pumping cycle, compression tests were conducted. It is likely that although the fibres within the collagen structure align and provide added strength in tension, they are weaker in compression, where the failure mechanism is likely to be strut buckling and pore

collapse. These porous structures are not as resistant to compressive deformation as tensile deformation, as found previously with scaffolds of other collagen-based composition (Huang et al. 2005). Where the gelatin scaffolds lacked stiffness in tension, the absence of stiff fibres allowed mechanical properties to be maintained in compression. Collagen-gelatin scaffolds show greatest promise since they are the only scaffold type whose compressive modulus does not vary significantly over the 14 days testing and thus maintain compressive strength even after degradation (~ 15% mass loss, Fig. 8a).

4.3 Insoluble versus Soluble Elastin

When using elastin as a substitute for type III collagen it must integrate well with the type I collagen or gelatin and possibly be able to form interfacial bonds with the collagen/gelatin. It was apparent in two compositions that this was not the case:

(1) Collagen-soluble elastin, where it is likely that the mass loss during crosslinking (11%, Table 2) represents a substantial proportion of the soluble elastin present. The reduced presence of globular soluble elastin in the crosslinked sample (Fig. 4 b and c) also confirms this, and indicates that the interaction between collagen type I and soluble elastin was not strong enough to retain the elastin within the scaffold (a possible lack of formation of inter-fibre bonds). These scaffolds showed reduced mechanical strength in both tension and compression compared with pure collagen due to lower protein content.

(2) Gelatin-insoluble elastin, where it is evident that the insoluble elastin fibres sank to the bottom of the scaffold and did not form a well dispersed mixture with the gelatin (Fig. 3 b). It was apparent that these fibres did not contribute to the bulk mechanical properties of the scaffold due to a reduced compressive stiffness compared with pure gelatin.

If either of these compositions (Coll-SE or Gel-IE) were to be used to produce a scaffold, alternative synthesis methods should be examined in order to produce an even dispersion of elastin throughout the scaffold that is retained after crosslinking. Good component interactions were seen in Coll-IE and Gel-SE samples; collagen can be seen trapping insoluble elastin and connecting separate elastin fibres (Fig. 3a), while in gelatin-soluble elastin the absence of obvious interfaces and no significant mass loss on crosslinking (only 2%) indicates a lack of phase separation. This is

consistent with the observations of Daamen *et al.* and Buttafoco *et al.* (Daamen et al. 2003; Buttafoco et al. 2005).

The tensile properties of the myocardium have been recorded over a range of values: stiffness at diastole (E=10–20 kPa) or systole (E=50–200 kPa (Nagueh et al. 2004; Alter et al. 2008; Engelmayr et al. 2008; Zhong et al. 2009; Wang et al. 2010)). The measured values of scaffold Young's modulus varied within this range depending on composition (Table 4). The addition of elastin to both collagen and gelatin scaffolds resulted in a slight increase in elongation at yield (in both tension and compression), which is expected due to its intrinsic elasticity. The tensile stress-strain curve of collagen-soluble elastin also closely matched that of the myocardium, which may be due to the loss of soluble elastin resulting in a scaffold with overall reduced collagen content. Collagen-insoluble elastin shows greater promise for use at high strains and would be preferable to one containing soluble elastin as the elastin is retained within the structure.

Since the pore size for the crosslinked scaffolds of different compositions is similar (130–160 μm, Table 2), and did not change throughout the duration of the swelling study (results not shown), it is expected that the uptake of PBS into the structure is similar for scaffolds of different composition. However, there was a slight increase in material and bulk fluid uptake by collagen-based scaffolds containing elastin compared with those not containing elastin, which may be as a result of the more hydrophilic nature of elastin. This was not the case for gelatin-based scaffolds, where the fluid uptake was similar for all compositions. It is likely that gelatin coats elastin, preventing additional swelling of the material.

Degradation studies in PBS demonstrated that the mass loss and change in compressive properties are dependent on the scaffold base composition and crosslinking. The stiffness of the scaffolds decreased after a time period of 10–14 days, closely matching the increasing loss of mass. Collagen containing insoluble elastin showed similar mass loss and compressive modulus to that of collagen, whereas collagen-soluble elastin had a significantly reduced compressive modulus; probably due to the loss of soluble elastin on crosslinking. In the case of gelatin, the layer of insoluble elastin fibres at the scaffold bottom are unlikely to have provided

any compressive stiffness, giving a lower modulus than pure gelatin. Where soluble elastin is present, scaffolds also appears to have a reduced compressive stiffness, possibly due to a reduced gelatin content and less stiff soluble elastin.

This is part of a larger programme of research that aims to first characterise scaffolds in terms of their bulk physical properties before investigating these properties at a cellular level. Although we have established that the composition most suitable for myocardial tissue engineering, in terms of morphological, mechanical and degradation properties, is one consisting of collagen (type I) containing insoluble elastin or gelatin and crosslinked, the exact composition can be tailored to match the properties of other soft tissues and be used in a wide range of applications. While the bulk properties are known, the properties at a cellular level still need to be investigated. Current investigations into the properties of thin films of these materials as well as their cell activity are underway, with the aim of producing a scaffold for use in soft tissue engineering that can be tailored to match both the bulk physical properties and remain biologically active.

5. Conclusion

In summary, varying the composition of a collagen- or gelatin-based scaffold alongside the use of crosslinking allows the physical properties to be better matched to those of the native heat tissue and show promise for use in other soft tissue engineering applications. Crosslinking is required for mechanical strength, enhanced fluid retention and degradation resistance, providing a scaffold with increased structural integrity. In using gelatin as a base-protein instead of collagen, the mechanical strength and stiffness and degradation resistance decreased, and therefore pure gelatin may be a suitable alternative to collagen for use in applications that require reduced stiffness and faster degradation rates e.g. skin repair. The addition of insoluble elastin to collagen scaffolds to mimic properties of type III collagen was successful in terms of mechanical and degradation properties. However, soluble elastin would not be recommended for future study, as a substantial proportion of the soluble elastin appeared to be lost during the crosslinking process. The combination of collagen and gelatin resulted in a scaffold that showed optimal mechanical and degradation properties. We have shown that varying the composition and cross-

linking of scaffolds allows their bulk properties to be altered and thus indicates they can be tailored to better suit their use in specific soft tissue engineering applications.

Acknowledgments

Funding for this study was provided by the Engineering and Physical Sciences Research Council.

The authors would like to thank Jeremy Skepper, of Cambridge University, for technical assistance with the fixing and SEM imaging of cell-seeded scaffolds.

References

Website: Last accessed Dec 2012 "Collagen Type III Price and Availability." from http://www.sigmaaldrich.com/catalog/ProductDetail.do?lang=en&N4=C4407|SIGMA&N5=SEARCH_CONCAT_PNO|BRAND_KEY&F=SPEC.

Alter PH et al., 2008 B-type natriuretic peptide and wall stress in dilated human heart. Mol Cellul Biochem 314, 179-191.

Bishop JER et al., 1990. Enhanced deposition of predominantly type I collagen in myocardial disease. J Mol Cellul Cardiol 22, 1157-1165.

Buttafoco LB et al., 2005. First Steps Towards Tissue Engineering of Small-Diameter Blood Vessels: Preparation of Flat Scaffolds of Collagen and Elastin by Means of Freeze Drying. J Biomed Mat Res 77, 357-368.

Charulatha V and Rajaram A 2003. Influence of different crosslinking treatments on the physical properties of collagen membranes. Biomaterials 24, 759-767.

Chiu LLY and Radisic M, 2010. Scaffolds with covalently immobilized VEGF and Angiopoietin-1 for vascularization of engineered tissues. Biomaterials 31, 226-241.

Chiu LLY et al., 2010. Bioactive Scaffolds for Engineering Vascularized Cardiac Tissues. Macromol Biosci 10, 1286-1301.

Daamen WF, et al., 2008. A Biomaterial Composed of Collagen and Solubilized Elastin Enhances Angiogenesis and Elastic Fiber Formation Without Calcification. Tissue Eng 14, 349-359.

Daamen WF et al., 2003. Preparation and evaluation of molecularly-defined collagen-elastin-glycosaminoglycan scaffolds for tissue engineering. Biomaterials 24, 4001-4009.

Daamen WF et al., 2007. Elastin as a biomaterial for tissue engineering. Biomaterials 28, 4378-4398.

Davidenko N et al., 2010. Collagen-hyaluronic acid scaffolds for adipose tissue engineering. Acta Biomaterialia 6, 3957-3968.

de Souza RR 2002. Aging of myocardial collagen. Biogerontology 3, 325-335.

Debessa CRG et al., 2001. Age related changes of the collagen network of the human heart. Mech Ageing Dev 122, 1049-1058.

Elliott JT et al., 2002. Thin Films of Collagen Affect Smooth Muscle Cell Morphology. Langmuir 19, 1506-1514.

Engelmayr GCM et al., 2008. Accordion-like honeycombs for tissue engineering of cardiac anisotropy. Nature Mat 7, 1003-1010.

Fujimoto KLK et al., 2007. An Elastic, Biodegradable Cardiac Patch Induces Contractile Smooth Muscle and Improves Cardiac Remodeling and Function in Subacute Myocardial Infarction. J Am Coll Cardiol 49, 2292-2300.

Fung YC 1993. Biomechanics: Mechanical Properties of Living Tissues, Springer US.

Gerdes AM et al., 1986. Regional differences in myocyte size in normal rat heart. Anat Rec 215, 420-426.

Geutjes PJ et al., 2007. From Molecules to Matrix: Construction and Evaluation of Molecularly Defined Bioscaffolds. Tissue Eng 585, 279-295.

Gosline JM et al., 2002. Elastic proteins: biological roles and mechanical properties. Philos Trans R Soc London: Biol Sci 357, 121-132.

Hafemann B et al., 2001. Cross-linking by 1-ethyl-3- (3-dimethylaminopropyl)-carbodiimide (EDC) of a collagen/elastin membrane meant to be used as a dermal substitute: effects on physical, biochemical and biological features in vitro. J Mater Sci: Mater M 12, 437-446.

Harley B et al., 2007. Mechanical characterization of collagen-glycosaminoglycan scaffolds. Acta Biomater 3, 463-474.

Hidalgo-Bastida LA et al., 2007. Cell adhesion and mechanical properties of a flexible scaffold for cardiac tissue engineering. Acta Biomater 3, 457-462.

Huang YS et al., 2005. In vitro characterization of chitosan-gelatin scaffolds for tissue engineering. Biomaterials 26, 7616-7627.

Jorge-Herrero EP et al., 1999. Influence of different chemical cross-linking treatments on the properties of bovine pericardium and collagen. Biomaterials 20, 539-545.

Kim BS and Mooney DJ 2000. Scaffolds for Engineering Smooth Muscle Under Cyclic Mechanical Strain Conditions. J Biomech Eng 122, 210-215.

Koshy SK et al., 2003. Collagen cross-linking: new dimension to cardiac remodeling. Cardiovasc Res 57, 594-598.

Kozlov PV and Burdygina GI 1983. The structure and properties of solid gelatin and the principles of their modification. Polymer 24, 651-666.

Lee CH et al., 2001. Biomedical applications of collagen. Int J Pharmaceutics 221, 1-22.

Li RK et al., 1999. Survival and Function of Bioengineered Cardiac Grafts. Circulation 100, 63-69.

Liu C et al., 2007. Design and Development of Three-Dimensional Scaffolds for Tissue Engineering. Chem Eng Res Des 85, 1051-1064.

Lowry et al. 1941. The determination of collagen and elastin in tissues, with results obtained in various normal tissues from different species. J Biol Chem 139, 795-804.

Madhavan K et al., 2010. Evaluation of composition and crosslinking effects on collagen-based composite constructs. Acta Biomater 6, 1413-1422.

Marijianowski MMH et al., 1995. Dilated cardiomyopathy is associated with an increase in the type I/type III collagen ratio: A quantitative assessment. J Am Coll Cardiol 25, 1263-1272.

Mukherjee D and Sen S 1991. Alteration of collagen phenotypes in ischemic cardiomyopathy. J Clin Invest. 88, 1141-1146.

Mukherjee D and Sen S 1993. Alteration of Cardiac Collagen Phenotypes in Hypertensive Hypertrophy: Role of Blood Pressure. J Mol Cellul Cardiol 25, 185-196.

Murphy CM et al., 2010. The effect of mean pore size on cell attachment, proliferation and migration in collagen-glycosaminoglycan scaffolds for bone tissue engineering. Biomaterials 31, 461-466.

Nagueh SF et al., 2004. Altered Titin Expression, Myocardial Stiffness, and Left Ventricular Function in Patients With Dilated Cardiomyopathy. Circulation 110, 155-162.

Norton GR et al., 1997. Myocardial Stiffness Is Attributed to Alterations in Cross-Linked Collagen Rather Than Total Collagen or Phenotypes in Spontaneously Hypertensive Rats. Circulation 96, 1991-1998.

O'Brien FJ et al., 2005. The effect of pore size on cell adhesion in collagen-GAG scaffolds. Biomaterials 26, 433-441.

Olde Damink LH et al., 1996. Cross-linking of dermal sheep collagen using a water-soluble carbodiimide. Biomaterials 17, 765-773.

Pauschinger et al., 1999. Dilated Cardiomyopathy Is Associated With Significant Changes in Collagen Type I/III ratio. Circulation 99, 2750-2756.

Pieper JS et al., 1999. Preparation and characterization of porous crosslinked collagenous matrices containing bioavailable chondroitin sulphate. Biomaterials 20, 847-858.

Radisic M and Vunjak-Novakovic G 2005. Cardiac Tissue Engineering. J Serb Chem Soc 70, 541-556.

Rosellini E et al., 2009. Preparation and characterization of alginate/gelatin blend films for cardiac tissue engineering. J Biomed Mat Res 91, 447-453.

van Luyn MJ et al., 2002. Cardiac tissue engineering: characteristics of in unison contracting two- and three-dimensional neonatal rat ventricle cell (co)-cultures. Biomaterials 23, 4793-4801.

Wang BA et al., 2010. Fabrication of cardiac patch with decellularized porcine myocardial scaffold and bone marrow mononuclear cells. J Biomed Mat Res 94, 1100-1110.

Weber KT. 1989. Cardiac interstitium in health and disease: the fibrillar collagen network. J Am Coll Cardiol 13, 1637-1652.

Xiang ZR et al., 2006. Collagen–GAG Scaffolds Grafted onto Myocardial Infarcts in a Rat Model: A Delivery Vehicle for Mesenchymal Stem Cells. Tissue Eng 12, 2467-2478.

Yamamoto KT et al., 2002. Myocardial stiffness is determined by ventricular fibrosis, but not by compensatory or excessive hypertrophy in hypertensive heart. Cardiovasc Res 55, 76-82.

Yang SH et al., 2005. Gelatin/chondroitin-6-sulfate copolymer scaffold for culturing human nucleus pulposus cells in vitro with production of extracellular matrix. J Biomed Mat Res 74, 488-494.

Zhong LY et al., 2009. Left ventricular regional wall curvedness and wall stress in patients with ischemic dilated cardiomyopathy. Am J Physiol Heart Circ Physiol 296, H573-584.

Zimmermann WH et al., 2002. Tissue Engineering of a Differentiated Cardiac Muscle Construct. Circ Res 90, 223-230.

Figure Captions

Table 1 Scaffold compositions and abbreviations.

Table 2 Morphological characteristics of the centre of scaffolds pre- and post-crosslinking. Note: * indicates statistically significant difference in comparison to non-crosslinked sample of same composition for statistical significance of $p \leq 0.05$ in Student's *t*-test, (n=10, data are mean ± SEM*).

Figure 1 Representative diagrams of component (phase) interactions in scaffolds; a) Coll, b) Coll-IE, c) Coll-SE, d) Gel, e) Gel-IE, f) Gel-SE and g) Coll-Gel. Collagen is represented by thick black fibres (indicating tensile strength), gelatin is dashed-line fibres (weaker and more easily dissolved), insoluble elastin fibres are thick and yellow, while soluble elastin is thinner and blue. IE mixes well with Coll and SE mixes well with Gel, whereas IE sinks in Gel scaffolds and SE forms globules on Coll fibres. Coll-Gel shows effective mixing.

Figure 2 SEM images of the cross-section and surfaces of a crosslinked collagen scaffold. a) Top, b) middle, c) bottom, d) top surface, e) bottom surface. Scale bar is 1mm.

Figure 3 SEM images of a) Coll-IE XL and b) Gel-IE XL scaffolds. a) Cross-section of the Coll-IE XL scaffold indicating a good interaction between elastin and collagen fibres; the collagen enwraps and bridges the elastin fibres. b) Base surface of the Gel-

IE XL scaffold, showing clumps of large elastin fibres that have not formed a homogeneous phase with the gelatin, but have instead sunk to the bottom of the scaffold. Scale bar is 10 μm.

Figure 4 SEM images of a) Coll-SE nX, b) Coll-SE XL and c) Gel-SE XL scaffolds. a) Arrows mark globules of soluble elastin, coating the collagen fibres, b) arrows point out the globules of soluble elastin that remain after crosslinking and c) single phase gelatin-soluble elastin scaffold. Scale bar is 10 μm.

Table 3 Number of moles of free amine groups per gram of film (x 10^5) in non- and crosslinked films and calculated degree of crosslinking. Note: ***** indicates statistically significant difference in comparison to non-crosslinked sample of same composition and ■ indicates significant difference between compositions for statistical significance of $p \leq 0.05$ (n = 4, data are mean ± SEM*).

Figure 5 Stress-strain curves in the physiological strain-regime for hydrated, crosslinked scaffolds tested in tension at 6 mm min^{-1} at room temperature. Three distinct regions: the toe, linear and failure regions can be identified. a) Collagen-based and mixed scaffolds, b) gelatin-based scaffolds. Representative uniaxial tensile stress-strain curve for full thickness left ventricular human myocardium (heart tissue) also shown (Nagueh, Shah et al. 2004).

Table 4 Mechanical Properties of crosslinked scaffolds, hydrated and tested in tension at 6 mm min^{-1} at room temperature and native myocardium (data obtain from (Nagueh, Shah et al. 2004; Alter, Rupp et al. 2008; Engelmayr, Cheng et al. 2008; Wang, Borazjani et al. 2010)). Note: ■ indicates significant difference between compositions (collagen-based and gelatin-based) for statistical significance of $p \leq 0.05$ (n = 9–12, data are mean ± SEM*).

Figure 6 Stress-strain curves for hydrated, crosslinked scaffolds tested in compression at 6 mm min^{-1} at room temperature. Distinct collapse plateau and densification regimes can be identified.

Figure 7 Comparison of fluid uptake of scaffolds of different composition and crosslinking. Time point data (graphs a and c) represent fluid uptake of the scaffold material after removal of pore water, and single column data (graphs b and d)

represent average fluid uptake of the scaffold as whole. a and b) Non-crosslinked and crosslinked collagen scaffolds, c and d) Collagen and Gelatin scaffolds. Note: * indicates statistically significant difference in comparison to non-crosslinked sample of same composition for statistical significance of $p \leq 0.05$ in Student's *t*-test, (n=4, data are mean ± SEM*).

Figure 8 Mass loss (a) and compressive modulus (b) of crosslinked scaffolds incubated in PBS at 37ºC for time period indicated, tested at 6 mm min^{-1}. Note: * indicates statistically significant difference in comparison to compressive modulus after 1 hour of scaffolds of the same composition for statistical significance of $p \leq 0.05$ in Student's *t*-test, (n=4, data are mean ± SEM*).

Figure 9 SEM image of HT1080 cells seeded in a crosslinked collagen-gelatin scaffold after culture for 3 days. Scale bars are a) 100 μm, b) 20 μm.

Figures

Table 1

Composition	Abbreviation Non-Crosslinked	Abbreviation Cross-linked
Collagen	Coll nX	Coll XL
Collagen + insoluble elastin (ratio 9:1)	Coll-IE nX	Coll-IE XL
Collagen + soluble elastin (ratio 9:1)	Coll-SE nX	Coll-SE XL
Gelatin	Gel nX	Gel XL
Gelatin + insoluble elastin (ratio 9:1)	Gel-IE nX	Gel-IE XL
Gelatin + soluble elastin (ratio 9:1)	Gel-SE nX	Gel-SE XL
Collagen + Gelatin (ratio 1:1)	Coll-Gel nX	Coll-Gel XL

Table 2

Composition	Porosity (%)	Pore Size (µm)	Shrinkage (%)	Mass Loss (%)
Coll nX	92	190 ± 20		
Coll XL	70 *	160 ± 10 *	19	2
Coll-IE nX	90	190 ± 20		
Coll-IE XL	78 *	160 ± 20	14	4
Coll-SE nX	88	180 ± 10		
Coll-SE XL	66 *	150 ± 15 *	19	11
Gel nX	85	150 ± 10		
Gel XL	69 *	130 ± 10	11	0
Gel-IE nX	84	160 ± 10		
Gel-IE XL	68 *	150 ± 15	15	1
Gel-SE nX	84	180 ± 10		
Gel-SE XL	65 *	160 ± 20	12	2
Coll-Gel nX	88	180 ± 20		
Coll-Gel XL	73 *	150 ± 20	22	3

Figure 1

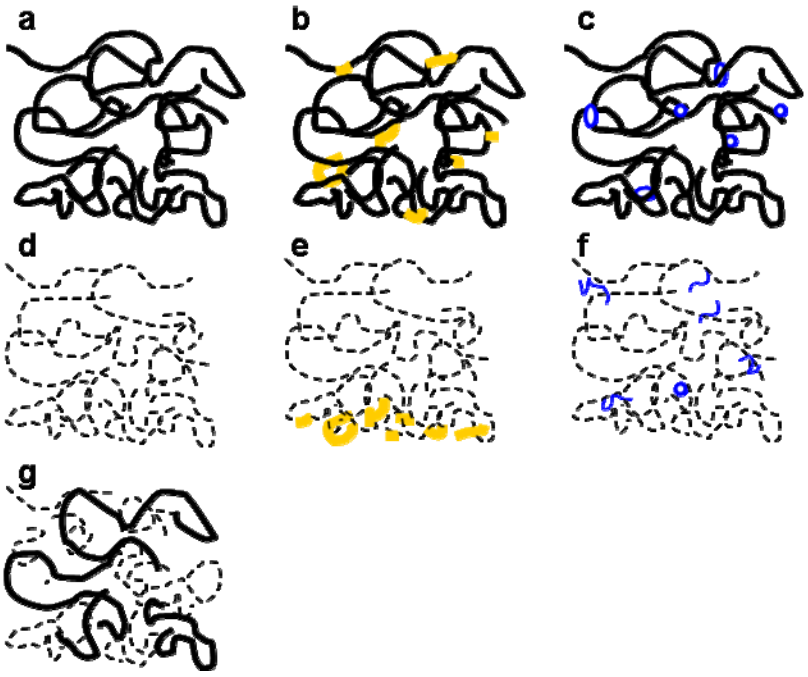

Figure 2

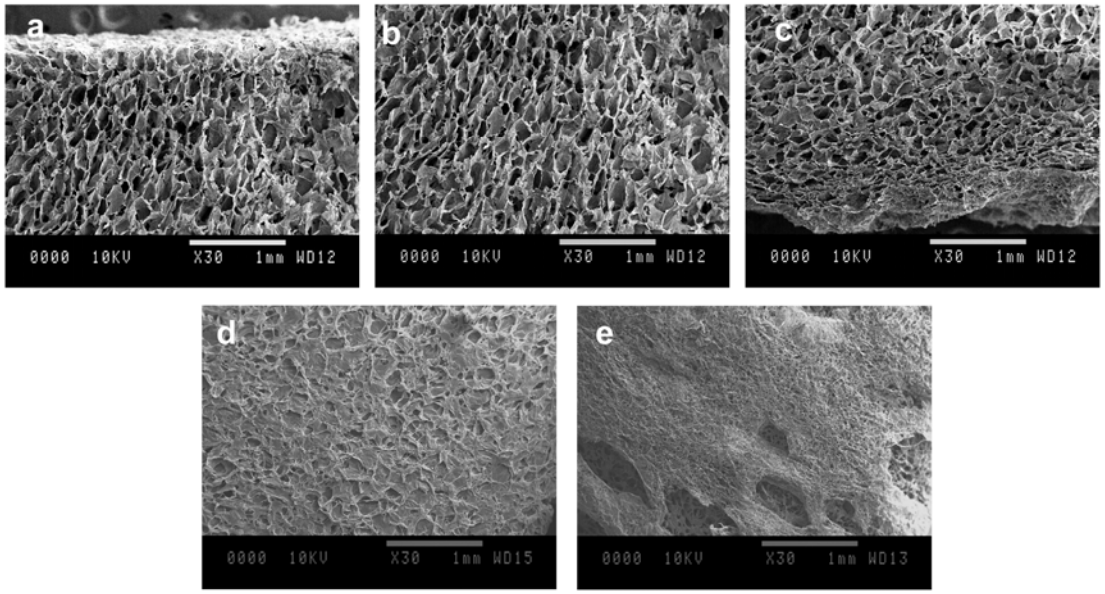

Figure 3

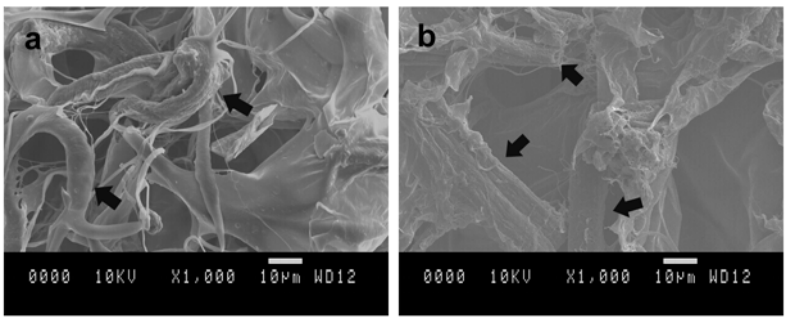

Figure 4

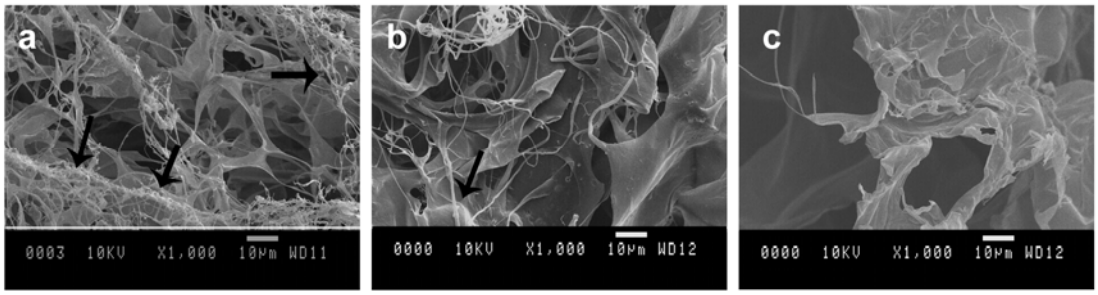

Table 3

	Uncross-linked	Cross-linked	Degree of Cross-linking
Coll	11 ± 0.27	4.5 ± 0.47 *	0.60 ± 0.14
Coll-IE	16 ± 0.70	8.6 ± 0.26 *	0.46 ± 0.08
Coll-SE	13 ± 0.54	6.3 ± 0.45 *	0.52 ± 0.12
Gel	21 ± 0.59 ■	8.4 ± 0.43 *	0.60 ± 0.06 ■
Gel-IE	25 ± 0.47 ■	6.2 ± 0.37 *	0.75 ± 0.06 ■
Gel-SE	21 ± 0.60 ■	4.5 ± 0.71 *	0.78 ± 0.09 ■
Coll-Gel	20 ± 0.47 ■	7.3 ± 0.28 *	0.64 ± 0.04

Figure 5

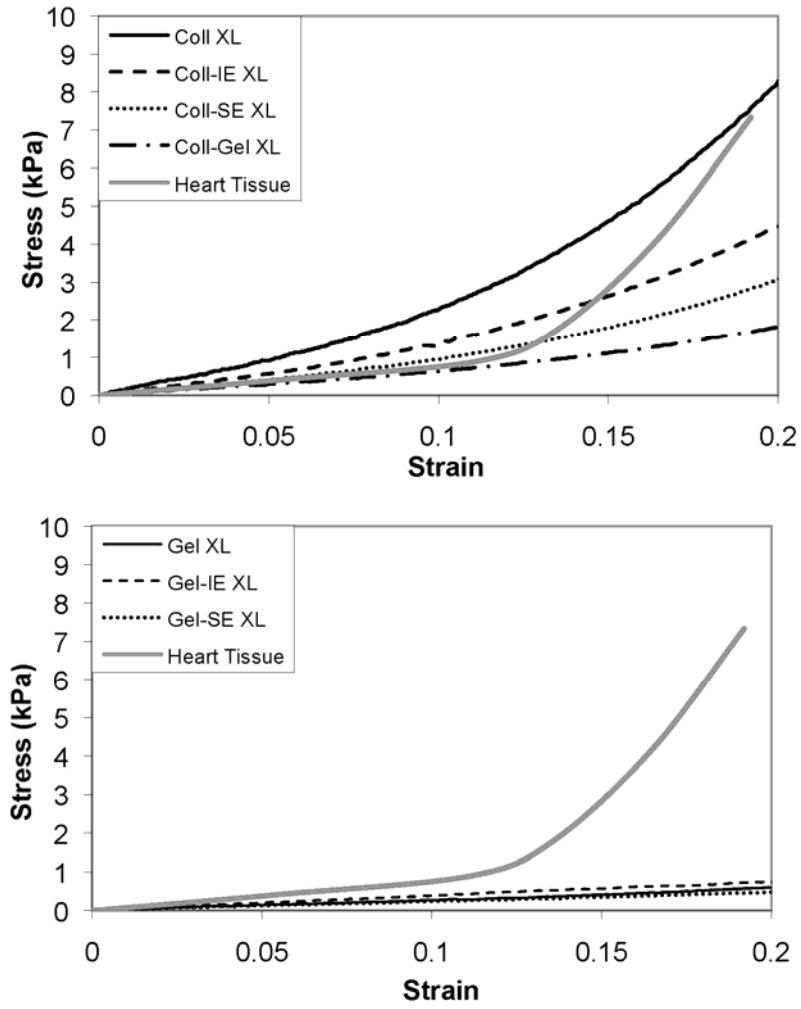

Table 4

	Strain at Failure	Stress at 20% Strain (kPa)	Youngs Modulus at 20% Strain (kPa)
Native Myocardium	-	4-20	24-150
Coll XL	0.32 ± 0.01	7.8 ± 0.9 ■	81 ± 8 ■
Coll-IE XL	0.33 ± 0.03	4.5 ± 0.8 ■	45 ± 9 ■
Coll-SE XL	0.41 ± 0.02	2.6 ± 0.2 ■	27 ± 2 ■
Gel XL	0.27 ± 0.05	0.75 ± 0.11	4.6 ± 0.1
Gel-IE XL	0.39 ± 0.03	0.77 ± 0.10	6 ± 1
Gel-SE XL	0.42 ± 0.03	0.36 ± 0.05	2.4 ± 0.2
Coll-Gel XL	0.42 ± 0.03	2.1 ± 0.3 ■	19 ± 3 ■

Figure 6

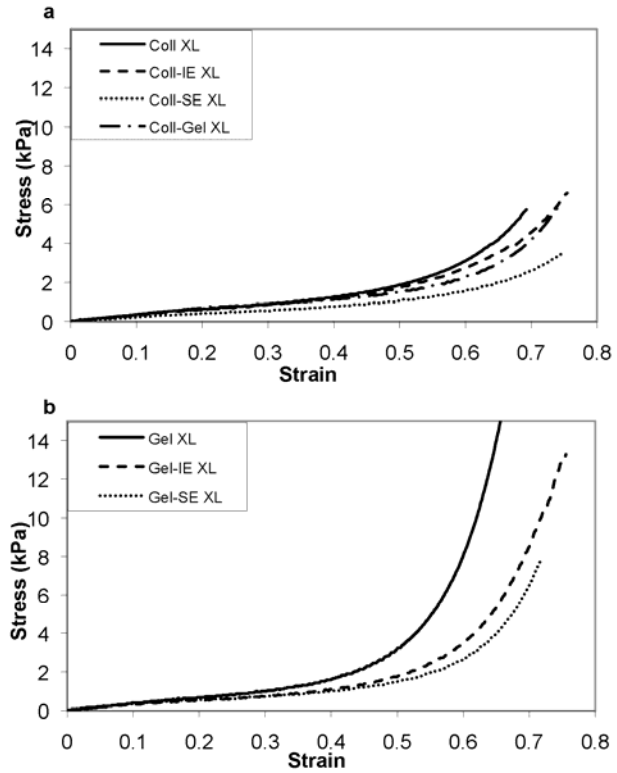

Figure 7

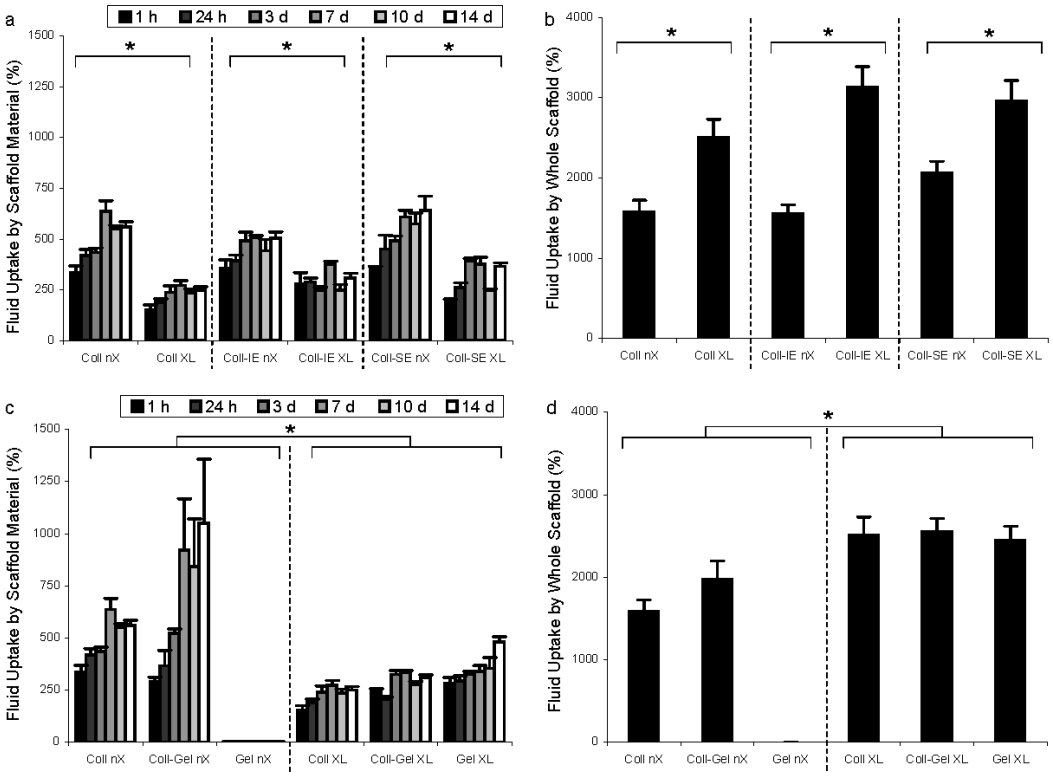

Figure 8

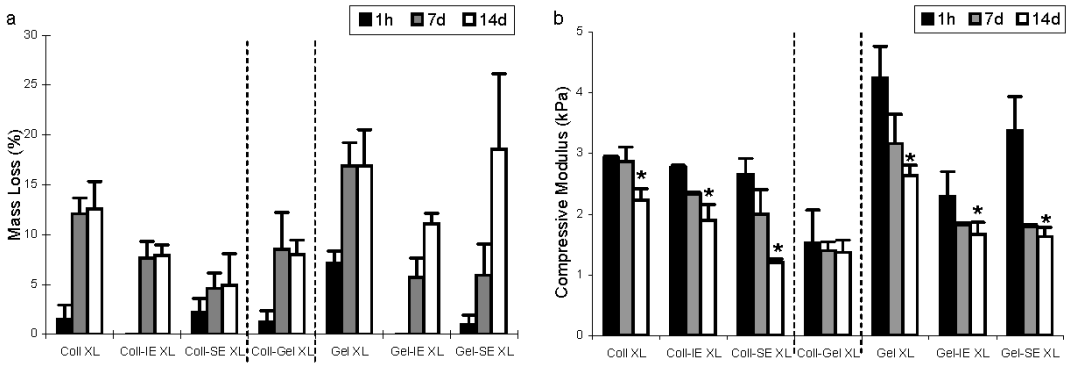

Figure 9